Applied Geochemistry 30 (2013) 4–15

Contents lists available at SciVerse ScienceDirect

Applied Geochemistry

journal homepage: www.elsevier.com/locate/apgeochem

Hydrogeochemical and isotopic evidence for trans-formational flow in a sedimentary basin: Implications for CO_2 storage

Fengtian Yang [a,b], Zhonghe Pang [a,*], Li Lin [c], Zhi Jia [c], Fengna Zhang [c], Zhongfeng Duan [d], Zhenhai Zong [c]

[a] Key Laboratory of Engineering Geomechanics, Institute of Geology and Geophysics, Chinese Academy of Sciences, Beijing 100029, China
[b] Key Laboratory of Groundwater Resources and Environment, Ministry of Education, Jilin University, Changchun 130021, China
[c] Tianjin Geothermal Exploration and Development-Designing Institute, Tianjin 300250, China
[d] School of Geosciences, China University of Petroleum (East China), Qingdao 266555, China

ARTICLE INFO

Article history:
Available online 5 September 2012

ABSTRACT

Deep saline aquifers are considered as the most promising option for geologic disposal of CO_2. One of the main concerns, however, is the integrity of the caprocks between and above the storage formations. Here, a hydrogeochemical and isotopic investigation is presented, using ionic chemistry, stable isotopes ($\delta^{18}O$, $\delta^{2}H$ and $^{87}Sr/^{86}Sr$) and radiocarbon dating, on five saline aquifers on a regional scale, namely: Neogene Minghuazhen, Guantao, Ordivician, Cambrian and Precambrian, all found in the Bohai Bay Basin (BBB) in North China. Groundwater recharge, flow pattern, age and mixing processes in the saline aquifers show that the Neogene Guantao Formation (Ng) in the Jizhong and Huanghua Depressions on both of the west and east sides of the Cangxian Uplift is a prospective reservoir for CO_2 sequestration, with a well confined regional seal above, which is the clayey layers in the Neogene Minghuazhen Formation (Nm). However, this is not the case in the Cangxian Uplift, where the Ng is missing where structural high and fault zones are developed, creating strong hydraulic connections and trans-formational flow to the Nm aquifer. Comparing storage capacity and long-term security between the various hydrogeologic units, the depressions are better candidate sites for CO_2 sequestration in the BBB.

1. Introduction

Deep saline aquifers are promising geological formations for long term sequestration of large quantities of CO_2 as a means of climate change mitigation (IPCC, 2005), since they offer the largest storage volume among all kinds of underground spaces for geological CO_2 sequestration and are widely distributed in sedimentary basins throughout the world (Koide et al., 1993). It is proposed that CO_2 be injected at depths greater than 800 m to be kept in supercritical state (Bachu, 2003). When injected into the formation, CO_2 spreads in the porous medium, displacing formation water and occupying an increasing portion of the flow domain (Pruess and Garcia, 2002), then being trapped through coupled physical and chemical mechanisms, including geological trapping (IPCC, 2005), hydrodynamic trapping (Bachu et al., 2007) and geochemical trapping (Gunter et al., 1997).

One of the major concerns for the sequestration is leakage of CO_2 from the reservoir. On a regional scale, the saline aquifer should be capped by an extensive aquitard or aquiclude to ensure CO_2 sequestration and to prevent it from escaping into adjacent formations or to the surface (Bachu, 2000). Crucial factors in determining the effectiveness of the caprocks include lithology, thickness, diagenesis, ductility, and local and regional continuity (Ho et al., 2005). There are several large Cenozoic–Mesozoic Basins in eastern China, such as the Songliao Baisin, BBB, Subei–Southern Yellow Sea Basin, East China Sea Basin and Pearl River Mouth Basin. These basins are characterized by high porosity and permeability, with good CO_2 source-sink matches and are potential areas for deployment of large scale CCS (Li et al., 2009; Pang et al., 2012), thus it is necessary to evaluate the confinement effectiveness of the saline aquifers in these basins.

In this study, Tianjin is taken as an example to carry out a primary characterization of the caprocks of the saline aquifers by examining the hydrodynamic regime of formation waters based on hydrogeochemical and isotopic data.

2. Geologic and hydrogeologic settings

Tianjin lies in the eastern part of the North China Plain, bordered by Beijing to the west, the Yanshan Mountains in Hebei province to the north and the Bohai Sea to the east with an area of 11,900 km^2 (Fig. 1). Tectonically, Tianjin is located at the northeastern part of the North China block, and is separated by the Baodi Fault into two sub-tectonic units (Fig. 1), the northern unit belonging to the Yanshan Folded Belt and the southern unit belonging to

* Corresponding author. Tel.: +86 010 8299 8613; fax: +86 010 6201 0846.
E-mail addresses: z.pang@mail.iggcas.ac.cn, pangzhonghe@gmail.com (Z. Pang).

0883-2927/$ - see front matter © 2012 Elsevier Ltd. All rights reserved.
http://dx.doi.org/10.1016/j.apgeochem.2012.08.024

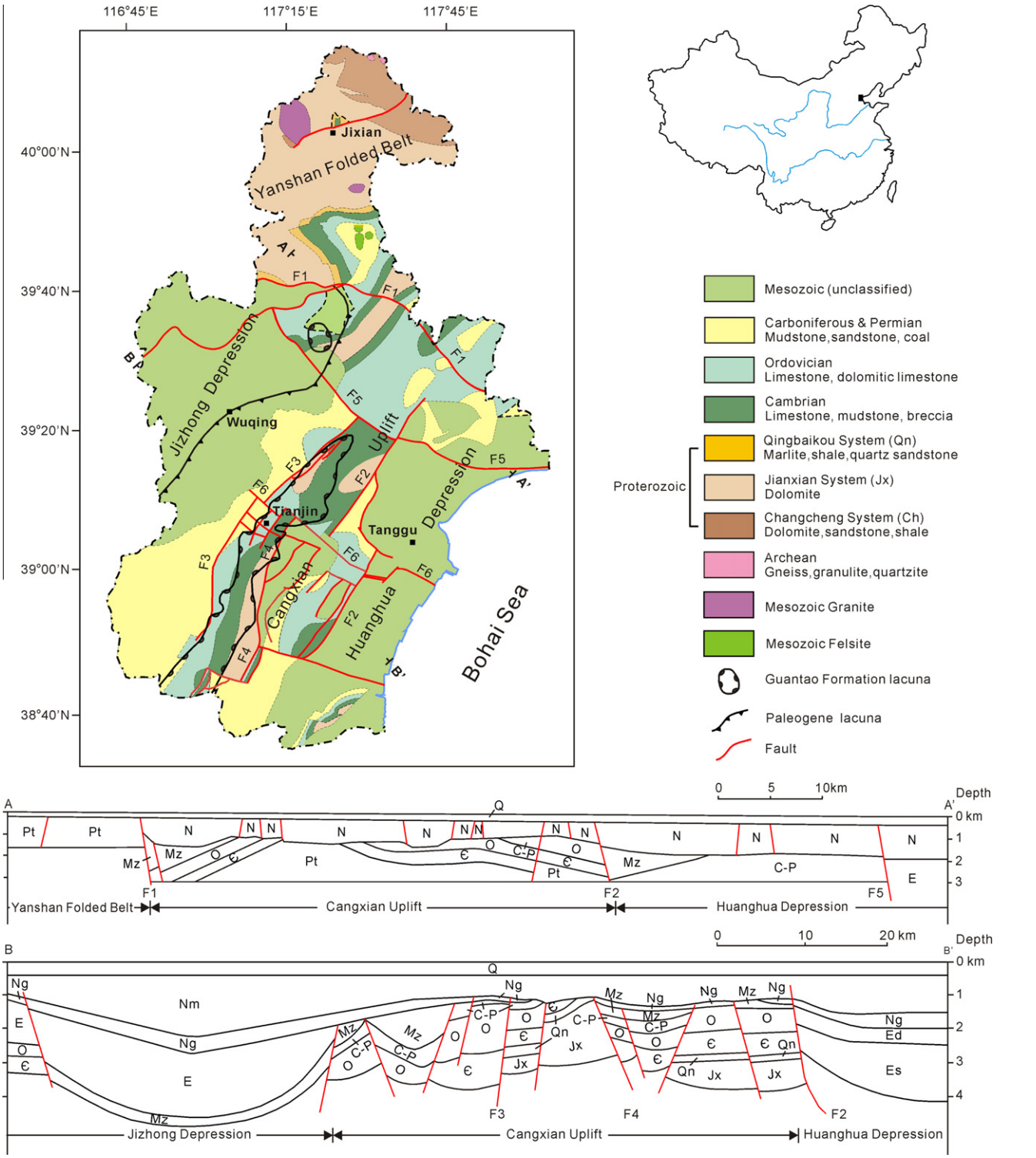

Fig. 1. Schematic geologic map of the substratum below the Cenozoic sediments, Tianjin. F1, Baodi Fault; F2, Cangdong Fault; F3, Tianjin Fault; F4, Baitangkou Fault; F5, Hangu Fault; F6, Haihe Fault.

the BBB, both of which are developed on the Archean basement of the North China Craton (Li, 1986; Liu et al., 1992; Allen et al., 1997).

The Achean system is composed of gneiss, granulite and quartzite, which constitute the local geologic basement, and is overlain by a Middle–Upper Proterozoic shallow water marine succession. The Phanerozoic system in the region is composed of Cambrian–Middle Ordovician shallow-marine carbonates, Upper Carboniferous–Lower Permian carbonates and coal-bearing clastics, Upper Permian–Triassic red beds and conglomerates, Jurassic coal-bearing clastics and continental volcano-sedimentary units which overlie older units unconformably (Davis et al., 2001), Cretaceous terrestrial volcanic rocks, volcaniclastic and clastic rocks, Eocene–Oligocene inland lacustrine sandstone and clay, Neogene fluvial and inland lacustrine sandstone, clay and Quaternary alluvial sandstone, clay and some marine deposits (Figs. 1 and 2).

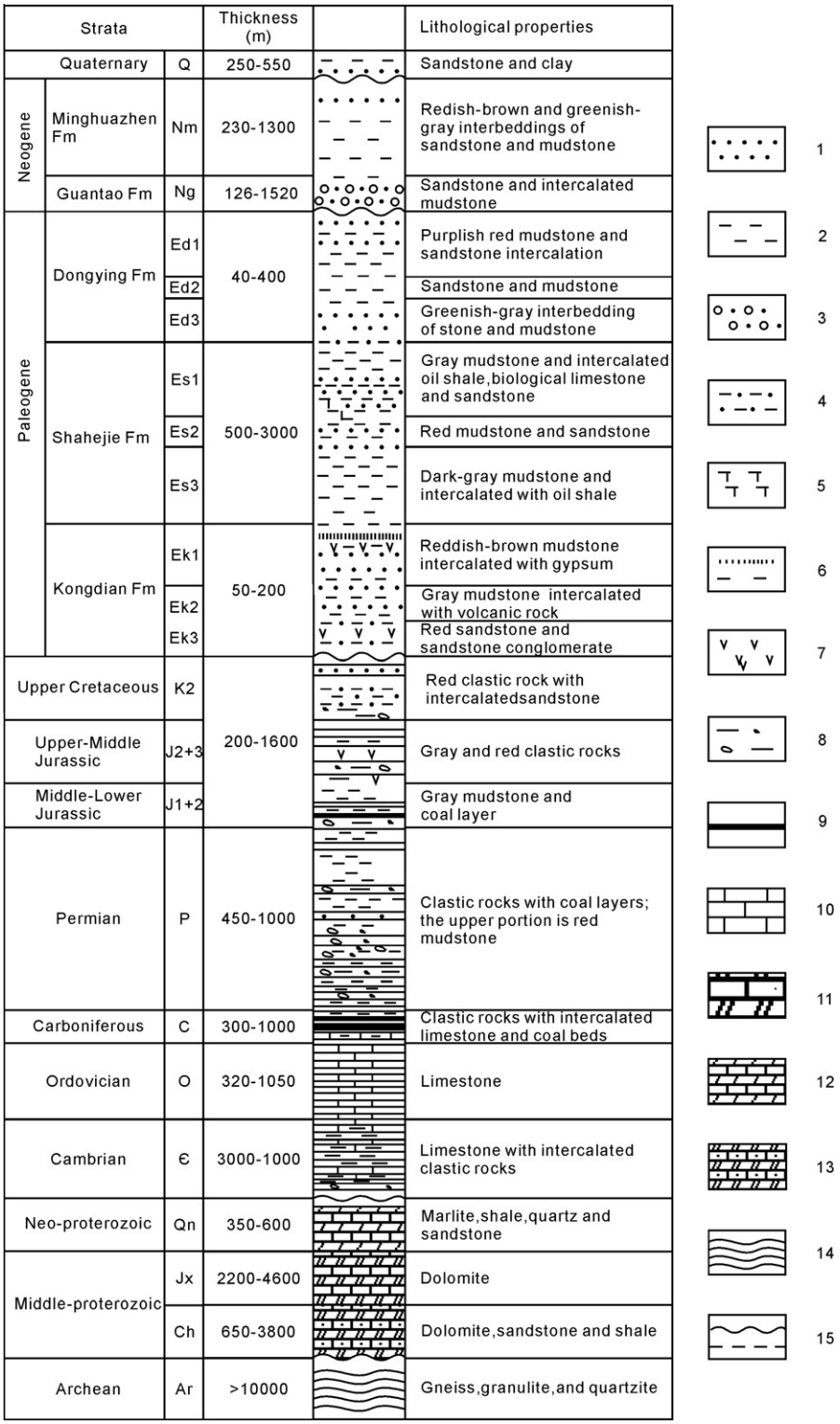

Fig. 2. A stratigraphic column of Tianjin (modified after Zhang et al., 2008) 1 = sandstone; 2 = mudstone; 3 = sandstone; 4 = oil shale; 5 = biological limestone; 6 = gypsum and conglomerate; 7 = volcanic rocks; 8 = clastic rocks; 9 = coal layer; 10 = lilmestone; 11 = dolostone; 12 = marlite; 13 = dolomite, sandstone and shale; 14 = metamorphic rock; 15=unconformity.

The northern unit of Tianjin in the Yanshan Folded Belt was uplifted in the Late Triassic–Early Cretaceous. The bedrocks are of Precambrian, Cambrian, Ordovician, Carboniferous and Permian, it outcrops to the north of Jixian (Fig. 1). To the south of Jixian, Quaternary sediment with a thickness of 100–300 m overlies the bedrocks unconformably, with no Paleogene or Neogene sediments. As the Quaternary sediment is too thin to be an effective seal, this unit is not discussed in the study. The southern unit of Tianjin in the BBB, which is a Cenozoic rifted intraplate basin, was developed in the Late Cretaceous and consists of a series of sub-basins, or Paleogene–Eocene rifts filled by a thick non-marine clastic succession (Li, 1986; Allen et al., 1997). A regional unconformity at the

top of the syn-rift sediments separates them from Neogene to recent strata, which were deposited during post-rift thermal subsidence (Hu et al., 2001).

The intense tectonic activity in the Mesozoic and Cenozoic have resulted in a structural setting of the BBB, which is dominated by two major fault systems, a NNE–SSW oriented alignment, which is transversely cut by the other tectonic lineament (Qi and Yang, 2010). There are several major faults in the southern unit, namely the Baodi Fault, Cangdong Fault, Tianjin Fault, Hangu Fault and Haihe Fault (Fig. 1). Among them, the Baodi Fault is a lithospheric fault, the others are crucial faults. The characteristics of the faults are summarized as follows.

The Baodi Fault strikes NW–NWW and dips SW–SSW, cutting into the Nm with a drop of ca. 40–400 m in the Nm, and controlling the distribution of the Mesozoic sediments (Fig. 1). The Cangdong Fault extends NNE and dips SEE, and cuts into the Nm. The drop of the fault is more than 1000 m in the Oligocene sediments (Fig. 1), ca. 200 m in the Ng and ca. 100 m in the Nm. Rocks to the west of the fault are of Precambrian and Paleozoic, while to the east of it they are mainly of Mesozoic and Cenozoic (Fig. 1). The Tianjin Fault strikes NNE and dips SSE, cutting into the Nm with a drop of ca. 60–300 m (Shao et al., 2010) (Fig. 1). The Baitangkou Fault strikes NNE and dips SSE, with a drop of 100–200 m. It cuts off the bedrocks, leading to the unconformable contact of the Neogene sediments with the Mesozoic strata to the east and the Middle–Upper Proterozoic strata to the west (Fig. 1). The Hangu Fault strikes NW–NWW and dips SW–SSW, The fault cuts into Nm with a drop of ca. 200 m and controls the distribution of the Paleoegene sediments. There is almost no Paleoegene to the north of the fault, while it is distributed widely to the south of it (Fig. 1). The Haihe Fault strikes NWW and dips SSW; it cuts into Ng with a drop of 80–100 m, controlling the development of the Mesozoic and Cenozoic sediments.

The NNE–SSW oriented faults form a horst–graben structure, which within Tianjin are the Cangxian Uplift in the center, the Huanghua Depression bordered by the Cangdong Fault to the east, and the Jizhong Depression bordered by the Paleogene lacuna to the west, all of which are bordered by the Baodi Fault to the north with the Yanshan Folded Belt. The bedrocks of the Cangxian Uplift are mainly of Middle–Upper Proterozoic and Paleozoic, with a buried depth of 1000–1600 m. The Mesozoic strata are mostly missing; the Ng is missing in the structural high from the central to the south, resulting in the direct contact of the Nm with the underlying pre-Cenozoic bedrocks. In the Jizhong and Huanghua Depressions, the bedrocks are of Middle–Upper Proterozoic, Paleozoic and Mesozoic; the thicknesses of the Cenozoic sedimentary series are 1200–9000 m and 900–5000 m in the Jizhong and Huanghua Depressions, respectively.

The regional hydrogeology, from the top to the bottom, can be summarized as follows: (i) the "Quaternary aquifer" consists of continental sediments with a thickness of 250–550 m, and stretches across the whole basin, forming a seal for the underlying Nm. It has been widely used for water supply. (ii) The "Neogene aquifers", including the Nm and Ng. The Nm covers the whole basin, with a thickness of 230–1300 m. It comprises continental clastic sediments and is sub-divided into two members. The upper member comprises siltstone inter-layered with mudstone and silty mudstone. The lower member dominantly comprises mudstones, inter-layered with fine sandstone. The sedimentary sequence clearly shows a fining upward point bar sequence deposited in a meandering river system. Since the upper member bears fresh groundwater and has been used for water supply, taking account of the risk of CO_2 leakage (Little and Jackson, 2010), the Nm is considered to be a potential regional seal rather than a reservoir. The Ng is distributed across the whole basin except for some areas in the structural high of the Cangxian Uplift (Fig. 1), with a thickness of 126–1520 m, comprising silty and fine sandstones inter-layered with mudstone in the upper and pebbled sandstone inter-layered with mudstone in the lower, and was deposited in a braided river system. It is characterized by high porosity and permeability, which are 18–36% and 1160–2000 $\times 10^{-3}$ mD, respectively. (iii) The "Paleogene aquifers", including the Dongying (Ed), Shahejie (Es) and Kongdian (Ek) Formations, mainly distributed in the Jizhong and Huanghua Depressions, with thicknesses of 3000–8000 m and 3000–5000 m, respectively. These aquifers are prospects for CO_2 sequestration, but are not discussed in this study due to a lack of data. (iv) The "Lower Paleozoic aquifers", including the Cambrian and Ordovician aquifers, which are located mainly in the Cangxian Uplift. The Cambrian aquifer has a thickness of 50–120 m and a buried depth of 1300–1800 m, while the Ordovician aquifer has a thickness of 450–750 m and a buried depth of 1000–2000 m (Lin, 2006). (v) The "Precambrian aquifers", including the Wumishan Formation of Jixian system (Jxw) and Qingbaikou system (Qn), with thicknesses of 2200–4600 m and 350–600 m, respectively, and buried depths of 910–3200 m. The Lower Proterozoic and Precambrian aquifers consist of limestone and dolostone. These rocks had undergone erosion and leaching due to regional uplift in the Middle Ordovician–Early Carboniferous and Mesozoic–Paleogene, accompanied by intense tectonic activities, and are characterized by karst and fracture-dominated secondary permeability (Zhai, 1997).

3. Sampling and analysis

Altogether chemical data on 170 samples are considered, among which 29 were collected from the geothermal production wells sunk in the Neogene aquifers in the Huanghua Depression and the Ordovician, Cambrian and Precambrian aquifers in the Cangxian Uplift during two sampling campaigns in December, 2009 and March, 2010, respectively. Analyses of water were conducted at the Analytical Laboratory, Beijing Research Institute of Uranium Geology, where anions ($F^-, Cl^-, SO_4^{2-}, NO_3^-$) were measured with a DIONEX-500 ion chromatograph, cations with an OPTIMA2X00/1500 ICP-OES and alkalinity using an automatic titrator (785DMP™). The other 140 samples were collected from shallow groundwater monitoring and thermal water exploration wells during 2001–2007 and the analyses were conducted at Tianjin Geology & Mineral Resources Experiment Center, where anions were measured with a DIONEX-ICS-1500 ion chromatograph, cations with an IRIS Intrepid II ICP-OES and alkalinity by titration. The methods for cation measurements were those of the National Analysis Standard DZ/T0064.28-93 and for anions DZ/T0064.51-93, while the same standard reference water samples distributed by the National Institute of Metrology, China were used. The analytical precision was 3% of concentration based on reproducibility of samples and standards and the detection limit was 0.1 mg/L. The charge balance error ranges from −5% to 5% for 163 samples and 5% to 19% for the other six samples which may have been caused by dilution or disturbance of organic matter. Another single sample is cited from Minissale et al. (2008), with a charge balance error of 1%.

Seven samples collected during the sampling campaigns were analyzed for $^{87}Sr/^{86}Sr$ ratios on a Finnigan MAT 262 thermal ionization mass spectrometer at the State Key Laboratory of Lithospheric Evolution, Institute of Geology and Geophysics, Chinese Academy of Sciences (IGGCAS), according to Xu and Han (2009). The Measured $^{87}Sr/^{86}Sr$ ratios were normalized against $^{86}Sr/^{88}Sr = 0.1194$ and the reported $^{87}Sr/^{86}Sr$ ratios were adjusted to the NBS SRM 987 standard $^{87}Sr/^{86}Sr = 0.71025$. The measurement precision is ±0.000015.

Stable water isotope composition on 16 groundwater samples were taken from Minissale et al. (2008) and on another 55 samples from both the sampling campaigns and the shallow groundwater monitoring and thermal water exploration. Twenty-nine water samples collected during the sampling campaigns were measured for $\delta^{18}O$ and $\delta^{2}H$ with a laser absorption water isotope spectrometer analyzer (Picarro L2120-i) at the Water Isotopes and Water–Rock Interaction Laboratory, IGGCAS. The results were reported with respect to the Vienna Standard Mean Ocean Water (VSMOW) in ‰ with precisions of ±0.2‰ and ±0.5‰ for $\delta^{18}O$ and $\delta^{2}H$, respectively, and the other 36 samples were measured at the Stable Isotopes Laboratory, IGGCAS with a Finnigan MAT 253 isotope ratio mass spectrometry by chrome reduction and equilibration with CO_2. The results were also reported against VSMOW in ‰ with precisions of ±0.02‰ and ±0.1‰ for $\delta^{18}O$ and $\delta^{2}H$, respectively.

Forty-two samples for ^{14}C and $\delta^{13}C$ in dissolved inorganic C (DIC) were collected in 2003 (Wang, 2005) and another 20 samples for ^{14}C and 9 for $\delta^{13}C$ were collected from the thermal water exploration wells. The DIC for ^{14}C determination was extracted as $BaCO_3$ from 100 L groundwater by adding $BaCl_2$ and CO_2-free NaOH solution to pH 10. Sample analyses using standard methods were performed at the Institute of Hydrogeology and Environmental Geology (IHEG), Chinese Academy of Geological Sciences. The ^{14}C activities of DIC were determined radiometrically by liquid

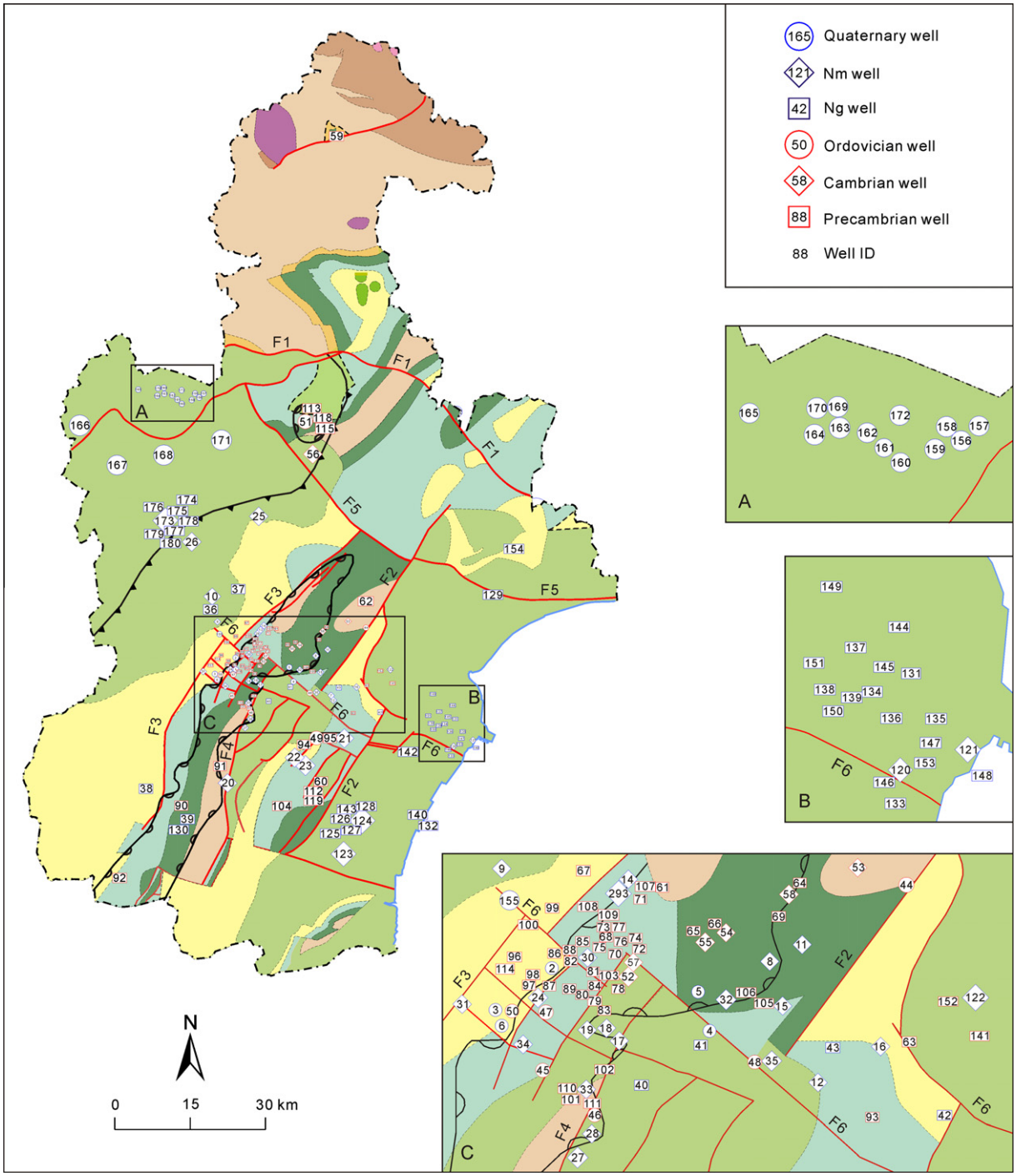

Fig. 3. Location of water sampling wells in Tianjin.

scintillation spectrometry (Quantulus™ 1220) with benzene as the scintillation solvent, the results being reported in pMC (percent modern carbon) with a measurement precision of ±0.3 pMC. The δ^{13}C-DIC was measured with a MAT 253 mass spectrometer at IHEG. The results are reported in ‰ deviations relative to the PDB (Pee Dee Belemnite) standard with precisions of ±0.1‰.

The location of the sampling wells is shown in Fig. 3 and the analytical results for the water samples are shown in Appendices A and B.

4. Discussion

4.1. Water isotopes and origin

Stable isotopes in the water samples from Tianjin are shown in Fig. 4. It is noted that all the samples plot to the right of the Global Meteoric Water Line (GMWL) and the Local Meteoric Water Line (Pang, 2000). Groundwaters from the Nm and Ng aquifers show relatively high δ^2H values with respect to those from the pre-Cenozoic aquifers, which may indicate a higher recharge elevation of the pre-Cenozoic aquifers. Using the relationship between isotopic composition and elevation for eastern China (Liu et al., 2010), the δ^2H values of the groudwaters suggest a similar origin, deriving from precipitation at elevations roughly between 1400 and 2400 m above sea level, perhaps in the Yanshan and Taihangshan Mountains to the North and NW of Tianjin, respectively. δ^2H values of all the water samples fall within a narrow range, i.e. between −76.7‰ and −68.0‰ VSMOW, whereas δ^{18}O values range widely, from −10.2‰ to −7.5‰ VSMOW, showing an "oxygen shift", which may be explained by the temperature effect of water–rock exchange. The "Oxygen shift" of the waters increases from the north to the south for each aquifer, indicating a groundwater flow direction from the north to the south.

4.2. Hydrochemistry and groundwater flow pattern

The chemical composition of water samples from the study area is plotted in a Schoeller diagram (Fig. 5). It shows that samples from the Quaternary aquifer have a TDS lower than 1000 mg/L and are of Na–HCO_3 type, except for one shallow water sample (#1) of Na–Cl type with higher TDS of up to 2300 mg/L, which was formed during the Late Quaternary marine transgression. Most

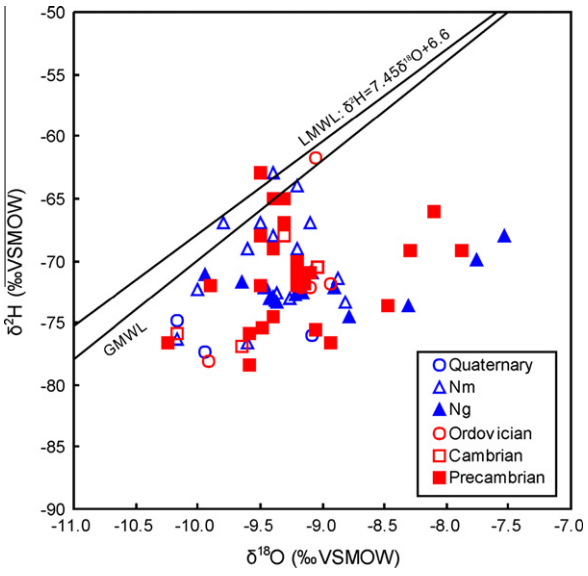

Fig. 4. Isotopic composition of groundwaters in Tianjin.

samples from the Neogene aquifers have a TDS of 800–1000 mg/L and are of Na–Cl–HCO_3 type, with a marked Na–HCO_3 component characteristic of lower TDS, i.e. 500–1000 mg/L. Samples from the underlying pre-Cenozoic aquifers have a higher TDS of 1400–1800 mg/L and are of Na–Cl type, except for one in the Yanshan Folded Belt (#59) and three samples in the northern part of the Jizhong Depression from the Ordovician (#51), Cambiran (#56) and Precambrian aquifers (#113), respectively, having a lower TDS of less than 900 mg/L and being of Na–HCO_3 type. Four samples from the Ordovician aquifer (#45, 46, 47 and 50) are of Na–SO_4 type, with a relatively high TDS of 3800–4500 mg/L and a high Ca content of 400–500 mg/L, which is an order of magnitude higher than those of the other waters.

Distribution of groundwater TDS and evolution of hydrochemical facies of the various aquifers were studied to determine the regional flow direction (Fig. 6). The TDS of the Nm aquifer increases from the NE to the SW (Fig. 6a) as the hydrogeochemical facies change gradually. In the Jizhong and Huanghua Depressions, TDS increase gradually from 500 to 2200 mg/L from the north to the south; groundwater evolves from HCO_3–Na type to Na–HCO_3–Cl and Na–Cl–HCO_3 types. In the area of the Cangixan Uplift where the Ng is missing or near the major faults, water from the Nm aquifer shows significant variations in TDS and water types. The lowest TDS is 690 mg/L (#78), while the highest reaches 3710 mg/L (#24). Various water types such as Na–HCO_3, Na–Cl–HCO_3, Na–HCO_3–Cl, Na–SO_4–Cl and Na–Cl–SO_4 exist, indicating mixing with groundwaters from the underlying pre-Cenozoic formations (as will be discussed below). TDS distribution of the Ng aquifer shows a similar pattern to that of the Nm (Fig. 6b). The groundwater in the northern part adjacent to the Yanshan Folded Belt has a TDS of <800 mg/L and is of a Na–HCO_3 type, towards the south, it gradually evolves into Na–HCO_3–Cl and Na–Cl–HCO_3 types, being characterized by a higher TDS of 1200–1900 mg/L. The TDS of water in the Ordovician aquifer also increases from the NE to the SW, however, with a large variation (Fig. 6c). The TDS of sample #51 in the northern Jizhong Depression is ca. 800 mg/L, while in the southeastern Huanghua Depression it is 39380 mg/L (Gao et al., 2010). The water chemistry is significantly affected by the Baitangkou Fault. Sample #44, 48 and 49 which are located to the east of the fault are of Na–Cl–HCO_3 type with a lower TDS of ca.1500 mg/L, while sample #45, 46, 47 and 50 to the west of it are of Na–Ca–SO_4–Cl type with a much higher TDS of 3900–4500 mg/L. Water samples from the Cambrian aquifer fall into two clusters, one is in northern Jizhong Depression with a TDS of less than 1000 mg/L and is characterized by a Na–HCO_3 type (#56), while the others in the Cangxian Uplift near the Haihe Fault have a higher TDS of ca. 1500 mg/L and are of Na–Cl type, with water chemistry similar to that form the local Precambrian aquifers. The TDS of the Precambrian aquifer increases gradually from less than 1000 mg/L in the north to more than 5000 mg/L in the south, while the water types evolve from Na–HCO_3 in the Yanshan Folded Belt and northern Jizhong Depression to Na–Cl–HCO_3 to the north of the Haihe Fault and Na–Cl–SO_4 to the south of the Haihe Fault (Fig. 6d). Thus, the spatial change of groundwater chemistry indicates that all the aquifers show a similar pattern in hydrochemical evolution, i.e. the goundwaters tend to evolve from Na–HCO_3 type to Na–Cl type as TDS gradually increases from the NE to the SW of the study area, indicating a NE–SW orientated flow path with the recharge area in the Yanshan Folded Belt, and flow towards the south.

4.3. Relationship between aquifers

Water samples were examined for the effects of possible mixing processes using both water chemical and isotopic methods.

Groundwaters from the Cenozoic and Pre-Cenozoic aquifers show different patterns of water chemistry between each aquifers

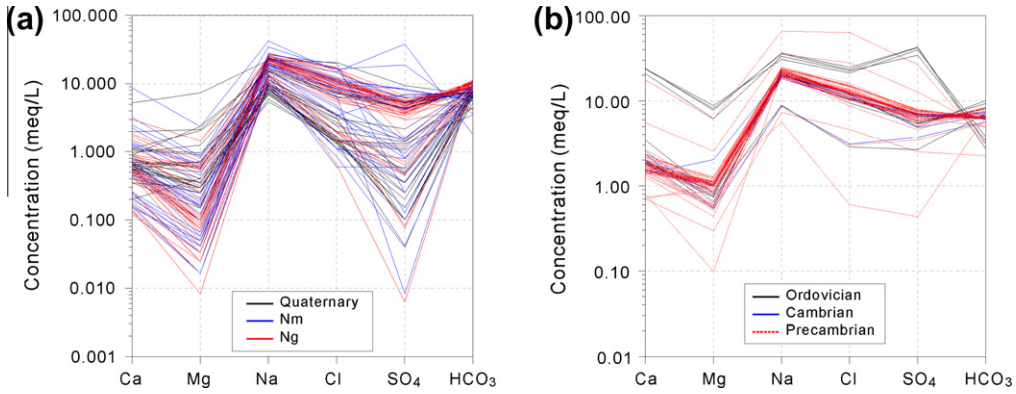

Fig. 5. Schoeller diagram for groundwaters in Tianjin. (a) Cenozoic aquifers; (b) Pre-Cenozoic aquifers.

(Fig. 5). Generally, groundwaters from the Pre-Cenozoic aquifers show a somewhat homogenous chemical composition in the center of the Cangxian Uplift (Fig. 5b). Waters with low TDS and Cl^- and SO_4^{2-} content only exist in the recharge area near the Yanshan Mountains, where water chemical compositions of the Precambrian (#113), Cambrian (#56) and Ordovician (#51) aquifers are nearly identical (Fig. 5b), indicating the same water origin. However, waters from the Precambrian (#90, 92) and Ordovician aquifers in the southern part of the Cangxin Uplift, have a much higher TDS (Appendix A, Fig. 3). As shown in Fig. 7, TDS at various depths of the pre-Cenozoic aquifers is quite uniform (1800–2000 mg/L), indicating a close hydraulic connection vertically in and between the aquifers as a result of well developed Karst and fractures in these aquifers and groundwater convection induced by a high geothermal gradient in the Cangxian Uplift (Minissale et al., 2008).

Groundwaters from the Neogoen aquifers show similar water types to those from the Pre-Cenozoic aquifers except for the ones in the north adjacent to the recharge area. Along the Cangdong, Haihe and Baitangkou Faults, groundwaters from the Neogene aquifers show higher TDS, while for those of the pre-Cenozoic aquifers show lower TDS (Fig. 6). This can be explained by the high permeability of the Cangdong and Haihe Faults. As shown in Fig. 8, the apparent ages of the groundwaters from the Precambrian aquifers become higher from the north to the south, indicating a southward groundwater flow. The ages along the Cangdong, Baitangkou and Haihe Faults are lower, and increase gradually further from the faults. Thus these are water-conducting faults.

These faults cut into the Neogene formations and result in their unconformable contact with the pre-Cenozoic formations. The $^{87}Sr/^{86}Sr$ ratios of the groundwaters (Fig. 9) show that the Sr concentrations and $^{87}Sr/^{86}Sr$ ratios of waters from the pre-Cenozoic aquifers are higher than those of the Neogene aquifers. The $^{87}Sr/^{86}Sr$ values for the pre-Cenozoic aquifers are between 0.70422 and 0.711025, except for one sample from the Ordorvician aquifer with a value of 0.708991, while for the Neogene aquifers they are between 0.708103 and 0.710753. As global ratios of marine carbonate range from 0.7060 to 0.7095 (Veizer et al., 1999), the observed trends associated with these $^{87}Sr/^{86}Sr$ ratios of the pre-Cenozoic aquifers, which is mainly comprised carbonate rocks, must reflect lithological control of the argillaceous and siliceous rocks contained in the formation or the underlying Achean crystalline basement. The waters from various aquifers along the Changdong and Haihe Faults form a mixing line, except for #50 from the Odorvician aquifer which may have mixed with another end member (as will be discussed below). The mixing trend is also confirmed by the relationship of δ^2H and the enthalpy of the groundwaters from both of the Neogene and pre-Cenozoic aquifers (Fig. 10). In the diagram the discharge enthalpies of the groundwaters are calculated from well head temperatures which would have only a minor uncertainty with respect to the reservoir temperatures, from monitoring experience, of ca. 1 °C/km. All the samples along the Cangdong, Haihe and Baitangkou Faults, especially in the area where the Changdong and the Haihe Faults cut each other fall on the same mixing line.

It is noted that water samples (#45, 46, 47 and 50) from the Ordovician aquifer in the structural high in the Cangxian Uplift where the Ng is missing show a distinct character of much higher TDS and SO_4^{2-} contents with respect to the others (Figs. 5 and 7). As shown in Fig. 11, the mass concentration ratio of TDS and Cl^- equals ca. 2.3 for the waters from the Neogene and pre-Cenozoic aquifers in the central area of the Cangxian Uplift, Jizhong and Huanghua Depressions. However, samples #45, 46, 47 and 50 from the Ordovician aquifer deviate from the line with increased TDS mainly caused by the increase in SO_4^{2-}. None of the Neogene, Ordovician, Cambrian and Precambrian aquifers have water of such a composition in the adjacent area, and the mineral compositions of the rock in the Ordovician aquifer does not change significantly with respect to the other Ordovician samples (Chen et al., 2009), thus there must be another mixing water member which is from the overlying or from the unconformable contact with the Upper Carboniferous–Lower Permian unites comprising carbonates and coal-bearing clastics (Evangelou and Zhang, 1995). Samples #20 and 24 in this area where the Ng is missing also show higher SO_4^{2-} content and the highest TDS of 2.5–3.6 mg/L among the water samples from the Nm aquifer, which may be caused by mixing with groundwater from the Ordovician aquifer as the two aquifers contact each other directly due to the Ng being missing.

4.4. Carbon isotopes and groundwater ages

Much of the DIC in groundwater derives from gaseous CO_2 in the vadose zone. This initial DIC containing high levels of ^{14}C is usually diluted by low ^{14}C activity DIC from mineral dissolution during groundwater recharge and flow. The large differences in $\delta^{13}C$ between the soil-derived DIC and carbonate minerals in the aquifer provide a reliable measure of the dilution. Carbonate dissolution during recharge continuously increases DIC and enriches the ^{13}C value. For ^{14}C age correction in this process, the Fonts–Garnier model (Fontes and Garnier, 1979) and Pearson model (Pearson and White, 1967) would be the representative of groundwater ages (Chen et al., 2003). Here, the ^{13}C-based Pearson model is used for age correction. Assuming soil CO_2 is taken up by the water without significant fractionation effects, the dilution factor q is given by

$$q = \left(\delta^{13}C_{DIC} - \delta^{13}C_{carb}\right)/\left(\delta^{13}C_{soil} - \delta^{13}C_{carb}\right)$$

where $\delta^{13}C_{DIC}$ is the measured $\delta^{13}C$ of DIC in groundwater, $\delta^{13}C_{soil}$ is the $\delta^{13}C$ of soil CO_2, and $\delta^{13}C_{carb}$ is the $\delta^{13}C$ of the calcite being dissolved.

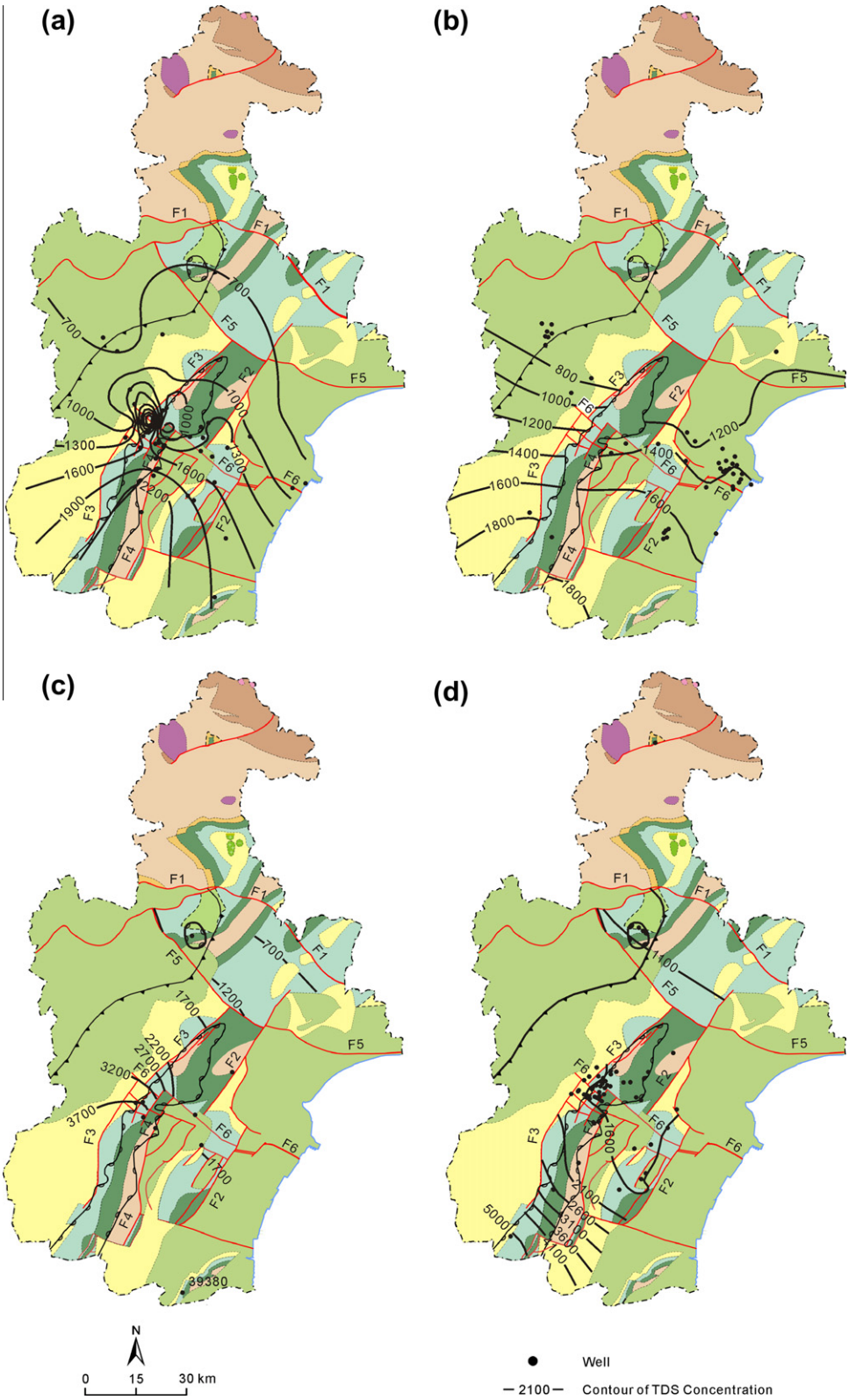

Fig. 6. Distribution of TDS for groundwaters in Tianjin. (a) Nm aquifer; (b) Ng aquifer; (c) Ordovician aquifer; (d) Precambrian aquifers.

With an estimated $\delta^{13}C_{soil}$ of −23‰ PDB and $\delta^{13}C_{carb}$ of 0‰ PDB, ages of the groundwaters are calculated (Appendix B, Fig. 12).

The result shows that waters from the Neogene aquifers generally have higher ages than those from the pre-Cenozoic aquifers. Groundwater ages for the Nm aquifer range between 13.6 and 24.0 ka B.P. The samples are in the Cangxian Uplift except for one in the Huanghua Depression, with an age of 17.1 ka B.P. For the Ng aquifer, groundwater ages fall between 8.4 and 20.2 ka B.P., i.e. 8.4–13.5 ka B.P. in the Cangxian Uplift, 12.8–15.4 ka B.P. in the Huanghua Depression and 10.7–20.2 ka B.P. in the Jizhong Depression.

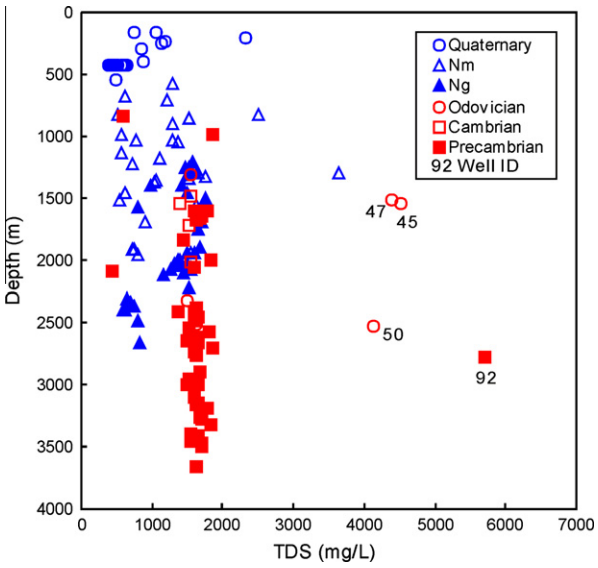

Fig. 7. TDS vs. depth for groundwaters in Tianjin.

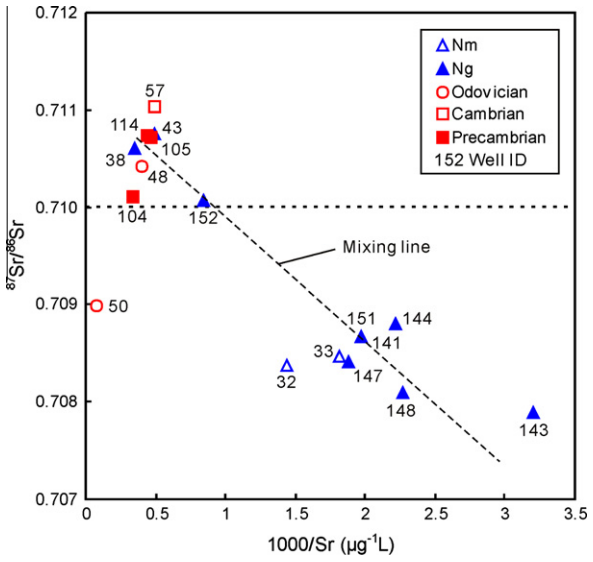

Fig. 9. Reciprocal of Sr concentration vs. $^{87}Sr/^{86}Sr$ ratio for groundwaters in Tian.

The pre-Cenozoic aquifers show lower values of groundwater ages. From the top to the bottom, the water ages increase. Groundwater from the Ordovician aquifer shows the lowest ages of 5.7–8.7 ka B.P., while the Precambrian aquifers show the highest of 5.8–18.2 ka B.P. Groundwater age of the Cambrian aquifer is 9.7–12.7 ka B.P., falling into the range of the Precambrian aquifers due to the close hydraulic connection between the two units.

It is noted that groundwater ages of the Ng aquifer are lower than those of the Nm aquifer in each structural units. The difference in groundwater ages demonstrates that there seems to be no significant groundwater mixing between the two aquifers, indicating the sealing effectiveness of the aquicludes between them.

4.5. Conceptual hydrogeologcial model

Based on the isotopic and chemical characteristics of the groundwaters in the southern unit of Tianjin in the BBB, the saline groundwaters receive recharge from precipitation in

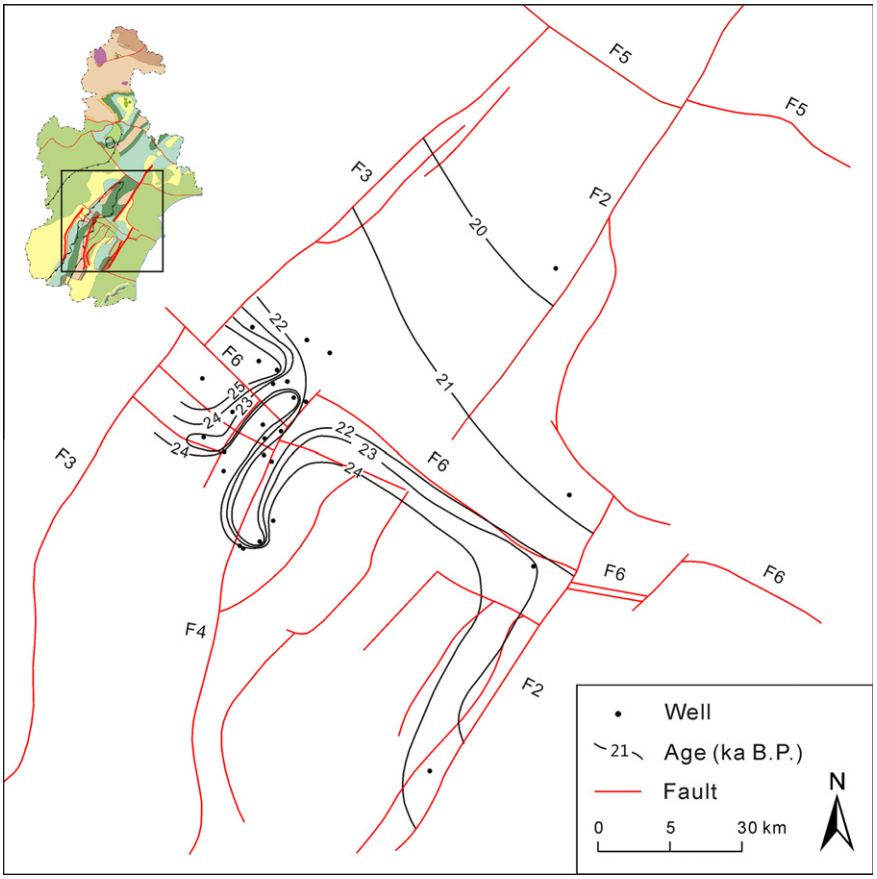

Fig. 8. Groundwater age of the Precambrian aquifers, Tianjin, showing preferential flows along the Cangdong, Haihe and Baitangkou Faults.

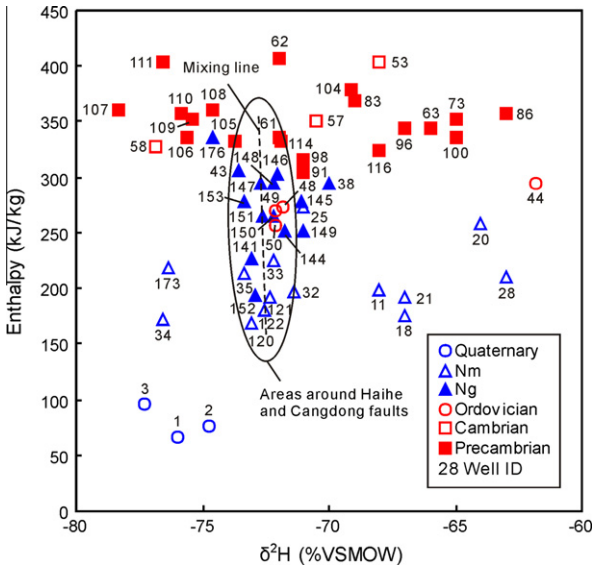

Fig. 10. δ^2H vs. enthalpy for groundwaters in Tianjin.

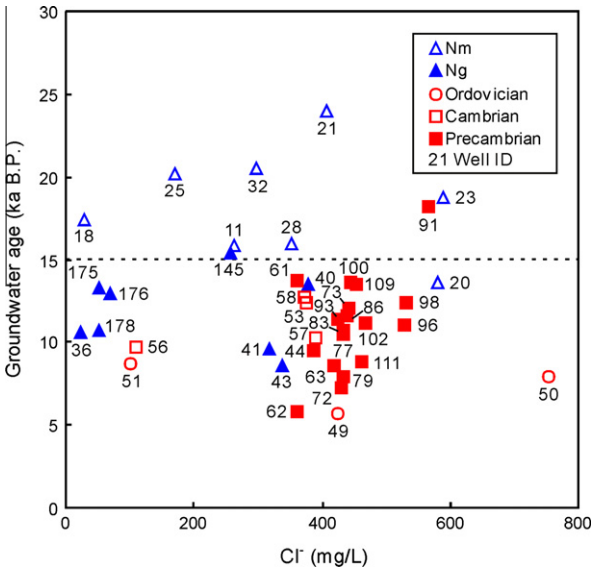

Fig. 12. Cl^- vs. ^{14}C age for groundwaters in Tianjin.

the Yanshan Mountains to the north and the Taihangshan Mountains to the NW. These waters are hosted in the continental Cenozoic sediments and the pre-Cenozoic carbonate-rich formations with different circulation velocities, and flow towards the south. Groundwaters in the Neogene formations move more slowly than those in the pre-Cenozoic ones, with ages of 8.4–24.0 ka B.P. and 5.7–18.2 ka B.P., respectively. As a result of well developed Karst and fractures in the pre-Cenozoic formations, these formations have close hydraulic connections. Due to the higher permeability along the Cangdong, Haihe and Baitangkou Faults, they form preferential pathways for groundwaters in the pre-Cenozoic formations. However, the Neogene formations have no significant connections with the underlying pre-Cenozoic formations except in the Cangxian Uplift where the water-conducting Cangdong, Haihe and Baitangkou Faults cut into the Nm and in the structural high where the Ng is missing. The conceptual model illustrating circulation of the saline waters in Tianjin is shown in Fig. 13.

4.6. Implications for CO_2 sequestration

The Nm forms a continuous cover in the BBB within the Tianjin area. Isotopic and chemical data show that there is little mixing between it and the underlying units except in the Cangxian Uplift along the Cangdong, Haihe and Baitangkou Faults and the structural high in the Cangxian Uplift where the Ng is missing, indicating the multi-layer mudstones in it act as impervious aquicludes. The groundwater age fall between 13.6 and 24.0 ka B.P., suggesting a low rate of water flow and relatively static hydrodynamics, which would preclude transport of CO_2 under hydrodynamic drive. Thus, it has the potential to act as a regional seal.

The Ng is distributed widely in the Jizhong and Huanghua Depressions and has no significant hydraulic connection with the overlying Nm. The water age ranges between 12.8 and 15.4 ka B.P., also implying an inactive water circulation and a semi-closed system (Zhou et al., 2008). With a high porosity and permeability of the formation, which has a good injectivity, a large thickness of 80–700 m, indicates

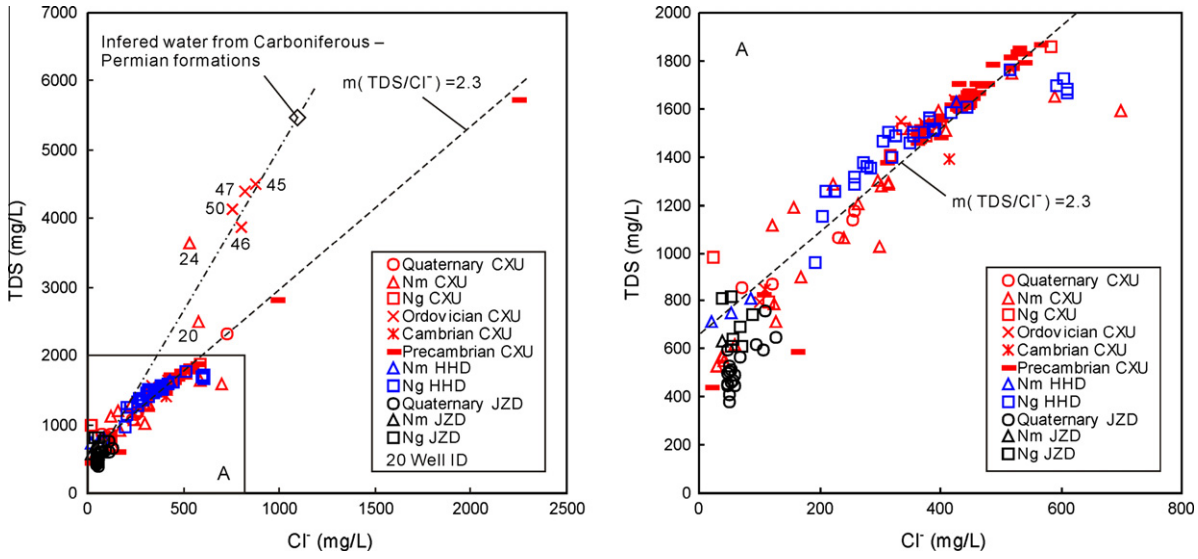

Fig. 11. Cl^- vs. TDS for groundwaters in Tianjin. CXU: Cangxian Uplift; HHD: Huanghua Depression; JZD: Jizhong Depression.

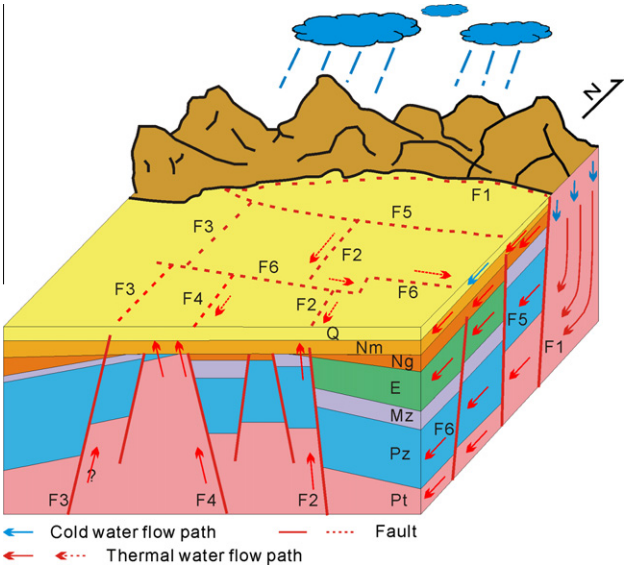

Fig. 13. Conceptual hydrogeologcial model for aquifers in Tianjin.

a huge capacity and an adequate buried depth between 1500 and 2700 m, and so is a prospective saline aquifer for CO_2 sequestration. However, as the formation is missing in the structure high, thus it is not suitable to be used in the Cangxian Uplift.

The pre-Cenozoic units in the Cangxian Uplift have closed hydraulic connections with each other through water-conducting faults which also cut into the Nm and have lead to water exchange between them, so CO_2 leakage may occur through the faulted zones. Moreover, these formations are characterized by high permeability resulted from well developed Karst and fractures, the water ages mostly range between 5.7 and 12.0 ka B.P., indicating a relatively fast water circulation, thus are not suitable for CO_2 sequestration.

5. Conclusions

Based on their hydrogeological and geochemical characteristics, the suitability of the saline aquifers in Tianjin was examined primarily from the circulation of the formation waters. The saline waters in the Neogene and pre-Cenozoic formations are recharged in the Yanshan Mountains to the north and the Taihangshan Mountains to the NW, with ages between 8.4–24.0 and 5.7–18.2 ka B.P., respectively, and flows from the north to the south.

The Cangdong, Haihe and Baitangkou Faults are water conductive, and form preferential pathways for the pre-Cenozoic formations, cut into the overlying Ng and Nm and result in hydraulic connections between them in the Cangxian Uplift.

The Nm is a potential regional seal except in the Cangxian Uplift where the Cangdong, Haihe and Baitangkou Faults cut into it and in the area of the structural high where the Ng is missing. The Ng shows no significant mixing with the overlying Nm in the Jizhong and Huanghua Depressions, and aquicludes in the Nm seem to be impervious, having the potential to be an effective regional seal.

The pre-Cenozoic units in the Cangxian Uplift are not suitable for CO_2 sequestration because the major faults such as the Cangdong, Haihe and Baitangkou Faults are water conductive and have cut into the overlying Nm, resulting in hydraulic connections between them and trans-formational flow to the Nm aquifer.

Acknowledgement

Funding for this work was provided by China National High-Tech R&D (863) Program (Grant 2008AA062303), which is gratefully acknowledged.

Supplementary material

Supplementary data associated with this article can be found, in the online version, at http://dx.doi.org/10.1016/j.apgeochem.2012.08.024.

References

Allen, M.B., Macdonald, D.I.M., Zhao, X., Vincent, S.J., Brouet-Menzies, C., 1997. Early Cenozoic two-phase extension and late Cenozoic thermal subsidence and inversion of the Bohai Basin, North China. Mar. Petrol. Geol. 14, 951–972.

Bachu, S., 2000. Sequestration of CO_2 in geological media: criteria and approach for site selection in response to climate change. Energy Convers. Manage. 41, 953–970.

Bachu, S., 2003. Screening and ranking of sedimentary basins for sequestration of CO_2 in geological media in response to climate change. Environ. Geol. 44, 277–289.

Bachu, S., Bonijoly, D., Bradshaw, J., Burruss, R., Holloway, S., Christensen, N.P., Mathiassen, O.M., 2007. CO_2 storage capacity estimation: methodology and gaps. Int. J. Greenh. Gas Control 1, 430–443.

Chen, Z.Y., Qi, J.X., Xu, J.M., Ye, H., Nan, Y.J., 2003. Paleoclimatic interpretation of the past 30 ka from isotopic studies of the deep confined aquifer of the North China plain. Appl. Geochem. 18, 997–1009.

Chen, R.J., Li, Y.Y., Tang, Y.X., Jia, Z., 2009. Analysis of causes and recharge–discharge of Ordovician geothermal fluid in Tianjin area. Global Geol. 28, 539–545.

Davis, G.A., Zheng, Y., Wang, C., Darby, B.J., Zhang, C., Gehrels, G., 2001. Mesozoic tectonic evolution of the Yanshan fold and thrust belt, with emphasis on Hebei and Liaoning Provinces, northern China. Geol. Soc. Am. Mem. 194, 171–197.

Evangelou, V.P., Zhang, Y.L., 1995. A review: pyrite oxidation mechanisms and acid mine drainage prevention. Crit. Rev. Environ. Sci. Technol. 25, 141–199.

Fontes, J.Ch., Garnier, J.M., 1979. Determination of the initial ^{14}C activity of total dissolved carbon: a review of existing models and a new approach. Water Resour. Res. 15, 399–413.

Gao, B.Z., Li, X.M., Zhi, Jia., Chen, R.J., 2010. Hydrogeochemical properties of the Tianjin (China) geothermal field. In: Proceedings of the World Geothermal Congress 2010, Bali, Indonesia.

Gunter, W.D., Wiwehar, B., Perkins, E.H., 1997. Aquifer disposal of CO_2-rich greenhouse gases: extension of the time scale of experiment for CO_2-sequestering reactions by geochemical modeling. Miner. Petrol. 59, 121–140.

Ho, A., Fokker, P.A., Orlic, B., 2005. Caprock Integrity of Deep Saline Reservoirs and Coupled Processes. Netherlands Institute of Applied Geosciences, Utrecht.

Hu, S.B., O'Sullivan, P.B., Raza, A., Kohn, B.P., 2001. Thermal history and tectonic subsidence of the Bohai Basin, northern China: a Cenozoic rifted and local pull-apart basin. Phys. Earth Planet. Int. 126, 221–235.

IPCC, 2005. IPCC Special Report on Carbon Dioxide Capture and Storage. Cambridge University Press, New York.

Koide, H.G., Tazaki, Y., Noguchi, Y., Iijirna, M., Ito, K., Shindo, Y., 1993. Carbon dioxide injection into useless aquifers and recovery of natural gas dissolved in fossil water. Energy Convers. Manage. 34, 921–924.

Li, D.S., 1986. The compounded geological characteristics of the Bohai Bay Basin. China Petrol. 7, 20–31.

Li, X.C., Wei, N., Liu, Y., Dahowski, R.T., Davidson, C.L., 2009. CO_2 point emission and geological storage capacity in China. Energy Procedia 1, 2793–2800.

Lin, L., 2006. Sustainable Development and Utilization of Thermal Groundwater Resources in the Geothermal Reservoir of the Wumishan Group in Tianjin. Ph.D. Dissertation, China Univ. Geosciences, Beijing.

Little, M.G., Jackson, R., 2010. Potential impacts of leakage from deep CO_2 geosequestration on overlying fresh water aquifers. Environ. Sci. Technol. 44, 9225–9232.

Liu, D., Nutman, A., Compston, W., Wu, J., Shen, Q., 1992. Remnants of 3800 Ma crust in the Chinese part of the Sino-Korean craton. Geology 20, 339–342.

Liu, J.R., Song, X.F., Yuan, G.F., Sun, X.M., Liu, X., Wang, S.Q., 2010. Characteristics of $\delta^{18}O$ in precipitation over Eastern Monsoon China and the water vapor sources. Chin. Sci. Bull. 55, 200–211.

Minissale, A., Daniele, B., Montegrossi, G., Aorlando, A., Tassi, F., Vaselli, O., Huertas, A.D., Yang, J.C., Cheng, W.Q., 2008. The Tianjin geothermal field (north-eastern China): water chemistry and possible reservoir permeability reduction phenomena. Geothermics. 37, 400–428.

Pang, Z., 2000. Isotope geochemistry of geothermal waters in northern China basin: implications on deep fluid migration. In: Proc. 2000 World Geothermal Congress, Kyushu-Tohoku, Japan.

Pang, Z., Li, Y., Yang, F., Duan, Z., 2012. Geochemistry of a continental saline aquifer for CO_2 sequestration: the Guantao formation in the Bohai Bay Basin, North China. Appl. Geochem. 27, 1821–1828.

Pearson, F.J., White, D.E., 1967. C-14 ages and flow rates of water in Carrizo Sand, Atascosa County, TX. Water Resour. Res. 3, 251–261.

Pruess, K., Garcia, J., 2002. Multiphase flow dynamics during CO_2 disposal into saline aquifers. Environ. Geol. 42, 282–295.

Qi, J.F., Yang, Q., 2010. Cenozoic structural deformation and dynamic processes of the Bohai Bay basin province, China. Mar. Petrol. Geol. 27, 757–771.

Shao, Y.X., Li, Z.H., Chen, Y.K., Ren, F., Yao, Z.Q., 2010. A study on the quaternary activity of Tianjin fault. Seismol. Geol. 32, 80–89.

Veizer, J., Ala, D., Azmy, K., Bruckschen, P., Buhl, D., Bruhn, F., Carden, G.A.F., Andreas, D., Ebneth, S., Godderis, Y., Jaspera, T., Kortea, C., Pawelleka, F., Fodlaha, A.G., Straussa, H., 1999. $^{87}Sr/^{86}Sr$, $\delta^{13}C$ and $\delta^{18}O$ evolution of Phanerozoic sea water. Chem. Geol. 161, 59–88.

Wang, K., 2005. Isotopic Geochemistry and Chronology Studies of Hydrogen, Oxygen and Carbon in Tianjin Geothermal Fluid. Ph.D. Dissertation. Peking Univ.

Xu, Z.F., Han, G.L., 2009. Chemical and strontium isotope characterization of rainwater in Beijing, China. Atmos. Environ. 43, 1954–1961.

Zhai, G.M. (Ed.), 1997. Petroleum Geology of China. Petroleum Industry Press, Beijing.

Zhang, T.W., Zhang, M.J., Bai, B.J., Wang, X.B., Li, L.W., 2008. Origin and accumulation of carbon dioxide in the Huanghua depression, Bohai Bay Basin, China. Am. Assoc. Petrol. Geolog. Bull. 92, 341–358.

Zhou, Q.L., Birkholzer, J.T., Tsang, C.F., Rutqvist, J., 2008. A method for quick assessment of CO_2 storage capacity in closed and semi-closed saline formations. Int. J. Greenh. Gas Control 2, 626–639.